MICROCOPY RESOLUTION TEST CHART
NATIONAL BUREAU OF STANDARDS 1963 A

BLOW-OFF PRESSURES FOR ADHERING LAYERS

by

A. N. Gent and L. H. Lewandowski

Institute of Polymer Science
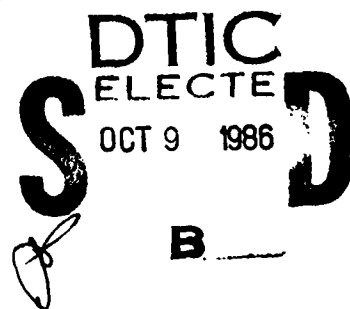The University of Akron
Akron, Ohio 44325

DTIC
ELECTE
OCT 9 1986
B

November, 1986

REPORT DOCUMENTATION PAGE		READ INSTRUCTIONS BEFORE COMPLETING FORM
1. REPORT NUMBER Technical Report No. 7	2. GOVT ACCESSION NO. AD-A172 997	3. RECIPIENT'S CATALOG NUMBER
4. TITLE (and Subtitle) Blow-Off Pressures for Adhering Layers		5. TYPE OF REPORT & PERIOD COVERED Technical Report
		6. PERFORMING ORG. REPORT NUMBER
7. AUTHOR(s) A. N. Gent and L. H. Lewandowski		8. CONTRACT OR GRANT NUMBER(s) N00014-85-K-0222
9. PERFORMING ORGANIZATION NAME AND ADDRESS Institute of Polymer Science The University of Akron Akron, Ohio 44325		10. PROGRAM ELEMENT, PROJECT, TASK AREA & WORK UNIT NUMBERS NR 092-555
11. CONTROLLING OFFICE NAME AND ADDRESS Office of Naval Research Power Program Arlington, VA 22217		12. REPORT DATE November, 1986
		13. NUMBER OF PAGES 35
14. MONITORING AGENCY NAME & ADDRESS(if different from Controlling Office)		15. SECURITY CLASS. (of this report) Unclassified
		15a. DECLASSIFICATION/DOWNGRADING SCHEDULE

16. DISTRIBUTION STATEMENT (of this Report)

According to attached distribution list.
Approved for public release; distribution unrestricted.

17. DISTRIBUTION STATEMENT (of the abstract entered in Block 20, if different from Report)

19. KEY WORDS (Continue on reverse side if necessary and identify by block number)

Adhesion, Blister Test, Bonding, Debonding, Detachment, Pressure Test, Tapes.

20. ABSTRACT (Continue on reverse side if necessary and identify by block number)

An analysis is given of the critical internal pressure P at which a circular debond ("blister") will grow in size, in terms of the tensile modulus E and thickness t of an adhering layer, and the strength G_a of its adhesion to a rigid substrate. Measurements of blow-off pressure are reported for adhering layers of pressure-sensitive tapes having widely-different effective modulus and thickness, and with blisters having a range of diameters. Satisfactory agreement is obtained with the theoretical

DD $_{1 \text{ JAN } 73}^{\text{FORM}}$ 1473   EDITION OF 1 NOV 65 IS OBSOLETE
S/N 0102-LF-014-6601

predictions, suggesting that the theory is basically correct in assuminc that relatively thin layers behave like elastic membranes. Attention is drawn to the unusual form of the dependence of the debonding pressure $\underline{P}$ upon the resistance $\underline{Et}$ of the layer to stretching and upon the detachment energy G_a: $P^4 \propto Et\ G_a^3$. Even though the adhering layer is assumed to be linearly-elastic, the markedly non-linear (cubic) relation between pressure $\underline{P}$ and volume $\underline{V}$ of the blister, or maximum height $\underline{y}$, leads to this unusual result. The detachment energy is given by a particularly simple function of the pressure $\underline{P}$ and maximum deflection $\underline{y}$ of the blister: $G_a = 0.65\ Py$, independent of the stiffness of the adhering layer and diameter of the blister.

Accession For

NTIS

DTI:

Uni:

Jus:

By

Dist:

Avail

Dist

A-1

1. Introduction

A pressurized blister test is a possible way of measuring the strength of adhesion between a deformable adhering layer and a rigid substrate. It was recommended by Dannenberg (1) and adopted by Williams and colleagues (2, 3) and Andrews and Stevenson (4) to study adhesion in selected systems. Interpretation of the measurements is not a simple matter, however. Three experimental situations can be distinguished: (i) the blister diameter is much smaller than the thickness of the adhering layer, (ii) the blister diameter is comparable to the thickness of the adhering layer, and, (iii) the blister diameter is much larger than the thickness of the adhering layer. Correspondingly, there are three different principal modes of deformation in the pressurized layer: (i) mainly in highly-stressed regions around the edge of the blister diameter, (ii) mainly in bending deformation of the adhesive layer, regarded as a flexible circular plate with a built-in edge constraint, and, (iii) mainly in tensile deformation of the adhesive layer, regarded as an elastic membrane.

In each case, by analysing the changes in stored elastic energy that take place as the blister grows and equating them to the energy required to separate the adhering layer from the substrate, values can be obtained for the critical pressure P for growth of the blister. In the first case, the result is (2, 5)

$$\text{(i)} \quad P^2 = 2\pi E G_a / 3a \tag{1}$$

and in the second case (6),

$$\text{(ii)} \quad P^2 = 128 \, E G_a t^3 / 9a^4, \tag{2}$$

where $\underline{E}$ denotes the tensile (Young's) modulus of the adhering layer, $\underline{G_a}$ is the energy required for detachment per unit of interfacial area (a measure of

the strength of adhesion), $\underline{a}$ is the radius of the blister, and $\underline{t}$ is the thickness of the deformable layer. For the third case, when the blister radius is relatively large compared to the layer thickness, the result, given in the Appendix, is

$$P^4 = 17.4 \, EG_a^3 t/a^4. \tag{3}$$

It is surprisingly different in form to the preceding results. The critical pressure is less strongly dependent upon the tensile modulus and thickness of the adhering layer and more strongly dependent upon the strength of adhesion than before. These marked differences arise from the different elastic response of a membrane to internal pressure in comparison with a plate. Deflections of a plate are directly proportional to the applied pressure, whereas deflections of a membrane are proportional to the one-third power of the inflating pressure (7) (it being assumed in both cases that the deflections are small).

In view of the serious consequences of delamination due to pressure in coatings and sealants, it is important to examine the validity of equation 3 thoroughly. Also, as suggested by Hinckley (8), a pressurized blister test may prove to be a good method of measuring interfacial adhesion. A detailed experimental study has therefore been carried out of the elastic deformation and critical debonding pressures for elastic layers adhering to rigid substrates. The layers consisted of commercial adhesive tapes, chosen for their widely-different elastic modulus. They were applied in multiple layers, so that the tensile stiffness of the composite layer could be changed substantially without any change in the strength of adhesion. They were also applied to two different substrates; Plexiglas and Teflon; so that the strength of adhesion could be changed (at least, in principle) without any

change in the elastic properties of the tape. The experimental procedures
and results are described below.

2. Experimental

Two commercial pressure-sensitive tapes were employed: $\underline{A}$, an electrical
tape with an acrylic adhesive layer and a soft vinyl backing, having a
thickness of about 0.18 mm (Tape No. 35, 3M Company); $\underline{B}$, a packing tape with
a biaxially-oriented polypropylene backing, having a thickness of about 0.09 mm
(Tape No. 375, 3M Company). They were chosen because they had similar
strengths of adhesion to Plexiglas and Teflon but quite different tensile
properties. As shown in Figure 1, tape $\underline{A}$ gave an approximately linear
relation between tensile stress and extension over the range 0 to 20 per cent
extension whereas tape $\underline{B}$ underwent plastic yielding at a tensile strain of
about 2-3 per cent. Below this strain, however, the stress-strain relation
was substantially linear and a value for the tensile stiffness $\underline{Et}$ per unit
width could be estimated. Experimentally-determined values at a rate of
extension of 1×10^{-6} s^{-1}, corresponding to the approximate rate of
extension in the blow-off experiments described later, were 900 ± 150 N/M
for tape $\underline{A}$ and 105 ± 15 kN/M for tape $\underline{B}$. Using the measured thicknesses $\underline{t}$,
these results correspond to effective values of tensile modulus $\underline{E}$ of 5.0 MPa
and 1.2 GPa, respectively.

The tapes showed some anisotropy in elastic behavior. Tape $\underline{A}$ was stiffer
in the machine direction in comparison with the transverse direction by about
30 per cent, whereas tape $\underline{B}$ was stiffer in the transverse direction by about
30 per cent. Values for $\underline{Et}$ given above are averages for the two directions.

A layer of each tape was adhered to a flat plate of Plexiglas containing
a central circular depression, about 1 mm deep and having a diameter of 25,

50 or 75 mm. The tape stretched over the circular depression without adhering to its base, so that an initial debond of well-defined shape and size was obtained. The depression was filled with a silicone vacuum grease also, to prevent any adhesion.

For studies of the elastic behavior, a rigid circular clamp was employed to secure the tape against the Plexiglas plate at the edge of the circular depression, Figure 2a. The effective diameter of the elastic membrane was then the same as that of the circular depression. In blow-off experiments this clamping ring was omitted, Figure 2b. Then, at a critical inflation pressure, further debonding took place at the edges of the circular depression. Measurements were made of the diameter, volume and height of the debonded region ("blister") and of the corresponding pressure required to make it grow, as the mean diameter of the blister increased from its initial value to a maximum value of about 75 mm.

The inflation pressure was measured using a mercury manometer for tape $\underline{A}$, and a calibrated Bourdon gauge for tape $\underline{B}$ when the values were considerably higher, approaching 1 atmos. The volume $\underline{V}$ of the blister was measured by metering the quantity of water injected into the debond through a small hole in the center of the circular depression, Figure 2. The deflection $\underline{y}$ of the center of the blister away from the undeformed plane was measured with a cathetometer. All measurements were carried out at ambient temperature, about 25°C, and at a rate of inflation of the blister of about 0.3 ml/min corresponding to a rate of growth of the blister radius of the order of 1 mm/min.

Peeling measurements were carried out at a peel angle of 90° and at the same rate, 1 mm/min, in order to determine the detachment energy G_a directly for each tape and substrate combination:

$$G_a = F/w \qquad (4)$$

where F is the peel force and w is the width of the tape.

3. Experimental Results and Discussion

Elastic behavior

When the radius of the blister was held constant by a clamping ring, Figure 2a, its volume V was found to be proportional to the deflection y of the center, as shown in Figure 3. Thus,

$$V = C_1 \pi a^2 y \qquad (5)$$

where πa^2 is the area debonded and C_1 is an experimentally-determined constant, 0.52, in good agreement with Hencky's theoretical result (7), given in the Appendix, $C_1 = 0.519$.

Experimental relations between inflation pressure P and maximum deflection y are given in Figure 4 for layers of tape A. Several layers were plied together to give a composite membrane with a tensile stiffness that was a simple multiple of the value for a single layer. The layers were secured with a clamping ring, as shown in Figure 2a, to hold the blister radius a constant during inflation. In each case the pressure P was found to be proportional to y^3, as shown in Figure 4, in good agreement with the theory of elastic membranes (see Appendix, equation A.2) and also proportional to the number N of layers plied together.

$$P = C_2' E t y^3 / a^4 \qquad (6)$$

From the slopes of the experimental relations, values of the tensile stiffness coefficient Et were calculated by means of equation A.2, using Hencky's value for the coefficient C_2' of 4.75 (7). The results were closely similar for blister radii of 12.5 and 25 mm: $Et = 1.01$ kN/m; and in good agreement with the value measured directly by tensile experiments on tape A, $Et = 0.90$ kN/m. Similar measurements with the stiffer tape B gave less satisfactory agreement, however. Values of Et of 45 ± 5 kN/m were deduced from inflation measurements using equation 6, whereas the directly measured value was considerably larger, 105 kN/m. This discrepancy may arise from difficulties in clamping the stiff tape B firmly at the edge of the blister during inflation experiments.

Debonding conditions

Typical experimental relations for tape B between inflating pressure P, maximum deflection y, and radius a, are shown in Figures 5 and 6. Initially, the membrane inflated into a blister with increasing height y with increasing pressure, but with the original radius a_0 of the circular debond. Then, at a critical pressure P_c, further debonding started and the pressure fell continuously as the blister grew in radius.

Actually, a small amount of debonding took place with increasing pressure, so that the radius of the initial blister grew by about 1 mm before the critical pressure was reached. After this, however, further growth of the blister took place with steadily-decreasing pressures, as the theory predicts (see Appendix). The anomalous behavior observed at the start is attributed to weak adhesion at the edges of the original blister, possibly due to entrapment of silicone grease there.

One of the theoretical predictions is that the product Py is a constant, directly related to the characteristic fracture energy G_a for the bond, equation A.9. The broken curve in Figure 5 is of this form, with the constant chosen to give best agreement with the experimental measurements. As can be seen, the experimental results agree reasonably well with the predicted dependence of P on the blister height y. Similarly, the broken curve in Figure 6 is of the theoretical form, equation A.10; Pa = constant; and again the constant has been chosen to give best agreement with the experimental measurements. And again the agreement is relatively good.

On the other hand, less satisfactory agreement was obtained with the softer tape A, as shown in Figures 7 and 8. During debonding the pressure P fell more rapidly as the blister height y and the radius a increased than an inverse proportionality would predict. This is attributed to a dependence of the fracture energy G_a upon the rate of detachment. During the blow-off experiments the effective rate of peeling changed, being initially more rapid and later slowing down, because of the way in which the experiments were conducted. The blister was inflated at a constant rate of volume increase, of about 0.3 ml/min, and not at a constant rate of increase of radius. Peel experiments revealed that the fracture energy for tape A depended strongly upon the rate of peel, increasing by about 50 per cent for a ten-fold increase in rate. Thus, the products Py and Pa would be expected to have larger values initially, and smaller values later, as was observed in the experiments, Figures 7 and 8, because of a continuous decrease in the effective peel rate.

Fracture energies

Average values of the products Py and Pa were obtained from experimental relations like those shown in Figures 5-8. They are listed in Table 1, together with values of the fracture energy G_a calculated from them by means of equations A.9 and A.10, respectively, using experimentally-determined values of the tensile stiffness coefficients Et in the latter case.

In all cases, values deduced for G_a from Pa and Py are seen to be in excellent agreement. They range from about 15 J/m^2 up to about 150 J/m^2, within the general range expected for pressure-sensitive adhesives, and they are distinctly smaller for a Teflon substrate, as would be expected. However, larger values were obtained by peeling strips of the same tapes away from the same substrates at 90°, given in the final column of Table 1. Similar discrepancies were noted before in comparing values of G_a obtained from pull-off experiments at shallow angles with those obtained from 90° peel tests (9). It was suggested then that the severe bending experienced by tapes in peeling at 90° may lead to additional energy being expended in dissipative processes. Further experiments are necessary to decide whether this factor is indeed responsible for the differences in G_a from the two types of detachment.

4. Conclusions

The following conclusions are obtained:

(i) Adhesive layers can be regarded as elastic membranes when a circular debond ("blister") at the interface is pressurized. As a result, the relation between inflation pressure and blister volume or blister height is approximately a cubic one until the blister starts to increase in radius by further debonding.

(ii) When an energy balance is applied to determine the conditions for growth of the blister by further debonding, a particularly simple relation is found to hold between the fracture energy G_a and the corresponding values of debonding pressure P and blister height y:

$$G_a = 0.65 \ Py,$$

independent of the radius of the blister or of the stiffness of the adhering layer.

(iii) Qualitatively similar conclusions were reached previously by Hinckley (8). The quantitative differences are discussed in the Appendix.

(iv) Measurements on two pressure-sensitive tapes, adhering to two different substrates, have been compared with the theoretical predictions. Although agreement is generally satisfactory, values deduced for the fracture energy G_a are consistently smaller than those obtained by peeling strips of the same tapes away from the same substrates at an angle of 90°. A similar discrepancy was noted in an

earlier study of detachment at shallow angles (9). It is provisionally attributed to additional energy dissipation in the tape backing when it is bent sharply away from the substrate at 90°.

Acknowledgements

References

1. H. Dannenberg, J. Appl. Polym. Sci. 5, 125-134 (1961).

2. M. L. Williams, J. Appl. Polym. Sci. 13, 29-40 (1969).

3. S. J. Bennett, K. L. DeVries and M. L. Williams, Int. J. Fracture 10, 33-43 (1974).

4. E. H. Andrews and A. Stevenson, J. Mat. Sci. 13, 1680-1688 (1978).

5. V. I. Mossakovskii and M. T. Rybka, PMM 28, 1061 (1964); J. Appl. Math. Mech. 28, 1277 (1964).

6. M. L. Williams, Proc. 5th U. S. Natl. Congr. Appl. Mech., Minneapolis, June 1966, A.S.M.E., New York, 1966, p. 451.

7. H. Hencky, Zeitschr. f. Math. u. Phys. 63, 311-317 (1915).

8. J. A. Hinckley, J. Adhesion 16, 115-126 (1983).

9. A. N. Gent and S. Y. Kaang, J. Appl. Polym. Sci., in press.

10. W. Z. Chien, Sci. Rep. Natn. Tsing Hua Univ. A5, 71-94 (1948).

11. R. W. Dickey, Arch. Ration. Mech. Anal. 26, 219-236 (1967).

12. R. Kao and N. Perrone, Int. J. Solids Structures 7, 1601-1612 (1971).

13. A. Kelkar, W. Elber and I. S. Raju, Computers and Structures 21, 413-421 (1985).

14. R. M. Christensen and W. W. Feng, J. Rheol. 30(1), 157-165 (1986).

Appendix

Theoretical relations for the deformation of a circular elastic membrane under a uniform pressure are reviewed below, and then employed to calculate the blow-off pressure for an adhesive layer containing a circular debond.

(i) Elastic deformation

Inflation of a thin circular elastic membrane, clamped at the periphery, has been analyzed by several authors. The results take the form:

$$V = C_1 \pi a^2 y \qquad (A.1)$$

and

$$y = C_2 (Pa^4/Et)^{1/3} \qquad (A.2)$$

where V is the volume of the "blister", y is the deflection of the center away from the membrane plane in the undeformed state, a and t are the radius and thickness of the membrane, E is Young's modulus for the membrane material, P is the inflating pressure and C_1 and C_2 are numerical coefficients whose values depend upon the value of Poisson's ratio v. Using series expansions, Hencky (7) obtained values of $C_1 = 0.518$ and $C_2 = 0.662$ for $v = 0.3$. Using his procedures, values of $C_1 = 0.519$ and $C_2 = 0.595$ are obtained when $v = 0.5$, i.e., for incompressible elastic layers, like rubber.

It should be noted, however, that other authors, using different starting points or purely numerical methods, have obtained slightly different values of C_2 than Hencky for $\nu = 0.3$: 0.653, 0.654 (10-13) but the same value when $\nu = 0.5$: $C_2 = 0.595$ (11). When the considerable approximation is made that the inflated membrane takes up the shape of a spherical cap, values of the coefficients are obtained that are at most only about 4 per cent smaller than Hencky's: $C_1 = 0.5$ for $\nu = 0.3$ or 0.5; and $C_2 = 0.640$ or 0.572 for $\nu = 0.3$ or 0.5, respectively (14).

Thus, there is a substantial level of agreement, although not complete, on the elastic deformation of an inflated membrane. In the analysis of debonding mechanics given below the deformation of the membrane is assumed to be that derived by Hencky.

(ii) Blow-off pressure.

An energy criterion for debonding is assumed to hold in which energy ΔW supplied to the system as the circular debond increases in radius by a small amount Δa is equated to energy expended in the debonding process itself. Changes in elastic energy in the membrane must also be taken into account. Thus,

$$\Delta W = \Delta W_1 + \Delta W_2 \qquad \text{(A.3)}$$

where the input energy $\Delta W = P\Delta V$, ΔW_1 denotes energy expended in detachment, given in terms of the characteristic energy G_a of detachment per unit area of bond by

$$\Delta W_1 = 2\pi a \, G_a \, \Delta a , \qquad \text{(A.4)}$$

and $\underline{\Delta W_2}$ denotes the change in energy stored elastically in the stretched membrane as the radius of the debond increases by an amount $\underline{\Delta a}$.

Input energy $\underline{\Delta W}$ is given by

$$\Delta W \equiv P(\partial V/\partial a)_p \, \Delta a = (10 \, PV/3a)\Delta a \qquad (A.5)$$

from equations A.1 and A.2.

On integrating the cubic relation between pressure and volume for a blister of constant radius $\underline{a}$, equations A.1 and A.2, the amount of energy stored in the inflated membrane is obtained as

$$W_2 = PV/4. \qquad (A.6)$$

Thus, as the radius of the blister increases by an amount $\underline{\Delta a}$ the energy term $\underline{W_2}$ changes by an amount:

$$\Delta W_2 = P(\partial V/\partial a)_p \, \Delta a/4 = \Delta W/4. \qquad (A.7)$$

On substituting from equations A.4, A.5 and A.7 in equation A.3, the detachment energy G_a is obtained as

$$G_a = 0.398 \, PV/a^2 \qquad (A.8)$$

or

$$G_a = 0.649 \, Py. \qquad (A.9)$$

The blow-off pressure is then obtained in terms of the blister radius $\underline{a}$ by means of equation A.2,

$$P^4 = 17.4 \, Et \, G_a{}^3/a^4. \qquad (A.10)$$

The main features of this analysis were recognized by Hinckley in 1983 (8): that the elastic behavior of an inflated blister follows membrane theory; that the relation between pressure $\underline{P}$ and deflection $\underline{y}$ will therefore be a cubic one; and

that an energy balance can be applied to determine the conditions
for growth of the blister by further debonding. However, the
treatment given here differs from that of Hinckley in two
respects: the approximation of the shape of the blister by a
spherical cap is not made; instead, the detailed analysis of
Hencky is employed; and, more importantly, the energy balance
given in equation A.3 is used in place of that proposed by
Hinckley, which takes the form

$$\Delta W_1 = \Delta W_2 \qquad (A.11)$$

in the present notation, and is thought to be incorrect. As a
result, Hinckley obtained the relation

$$G_a = 0.25 \ Py \qquad (A.12)$$

in place of equation A.9.

Table 1: Fracture energies G_a (J/m²) from blow-off and from peeling experiments.

| Number N of layers	$\frac{Pa}{}$ (N/m)	$\frac{Py}{}$ (N/m)	$\frac{G_a}{}$ (calc. from $\underline{Pa}$)	$\frac{G_a}{}$ (calc. from $\underline{Py}$)	$\frac{G_a}{}$ (from peeling)
			Tape $\underline{A}$ on Plexiglas substrate		
1	129 ± 11	38 ± 5	26 ± 3	24.5 ± 3	45.2 ± 3
2	155 ± 13	38 ± 3.5	26.5 ± 3	24.5 ± 2.5	
3	165 ± 27	36 ± 7	24.5 ± 5.5	23.5 ± 4.5	
5	175 ± 25	33 ± 6	23 ± 4.5	21.5 ± 3.5	
7	190 ± 15	32 ± 3.5	22.5 ± 2.5	20.8 ± 2.1	
10	195 ± 25	32 ± 5	21 ± 3.5	20.8 ± 3.4	
			Tape $\underline{A}$ on Teflon substrate		
1	101 ± 7	22.3 ± 2.5	18.5 ± 2	14.5 ± 1.5	46.2 ± 1.5
			Tape $\underline{B}$ on Plexiglas substrate		
1	1575 ± 65	237 ± 12	150 ± 8	154 ± 8	228 ± 12
			Tape $\underline{B}$ on Teflon substrate		
1	375 ± 10	41.5 ± 1.5	22.2 ± 1	26.9 ± 1	95.5 ± 6

Figure Captions

1. Relations between tensile force per unit width F/w and extension e for tapes A and B.

2. (a) Measurement of elastic behavior of a pressurized membrane, radius a_0.

   (b) Measurement of blow-off pressures and deflections.

3. Experimental relation between blister volume V and height y for clamped layers having a radius a_0 of 38 mm. O, two layers of tape B; $\triangledown$, 5 layers of tape A.

4. Experimental relations between inflation pressure P and blister height y for clamped layers of tape A having a radius a_0 of 25 mm. N denotes the number of layers plied together.

5. Experimental relation between inflation pressure P and maximum height y of the blister for one layer of tape B. The broken curves are of the theoretical forms: $P \propto y^3$, equation A.2, for inflation; and $P \propto 1/y$, equation A.9, for debonding.

6. Experimental relation between inflation pressure P and blister radius a for one layer of tape B. The broken curve is of the theoretical form, equation A.10, Pa = constant.

7. Experimental relation between inflation pressure P and maximum height y of the blister for one layer of tape A with an initial debond radius a_0 = 12.5 mm. The broken curve is of the theoretical form; Py = constant, equation A.9.

8. Experimental relation between inflation pressure P and
   blister radius a for one layer of tape A. The broken curve
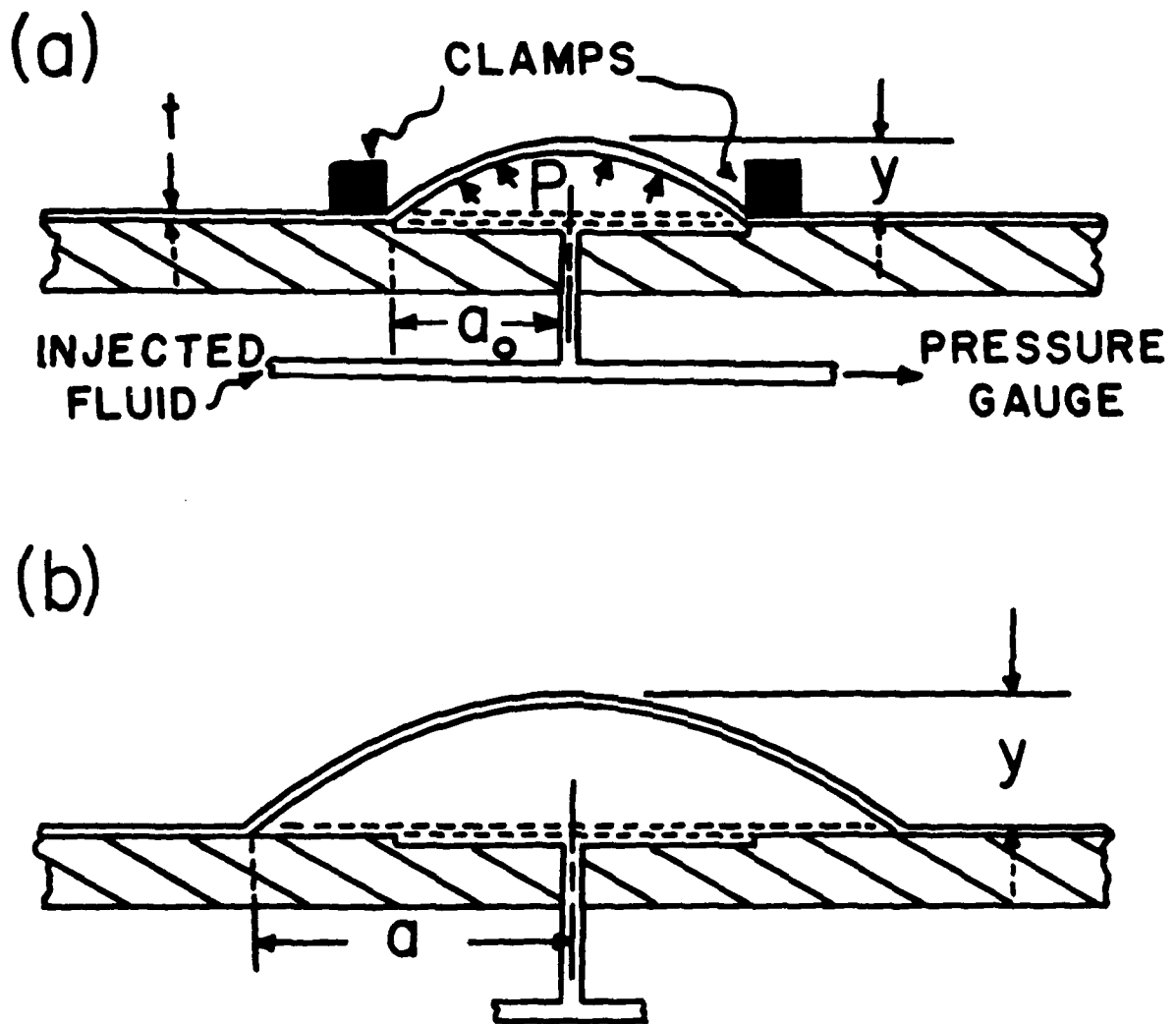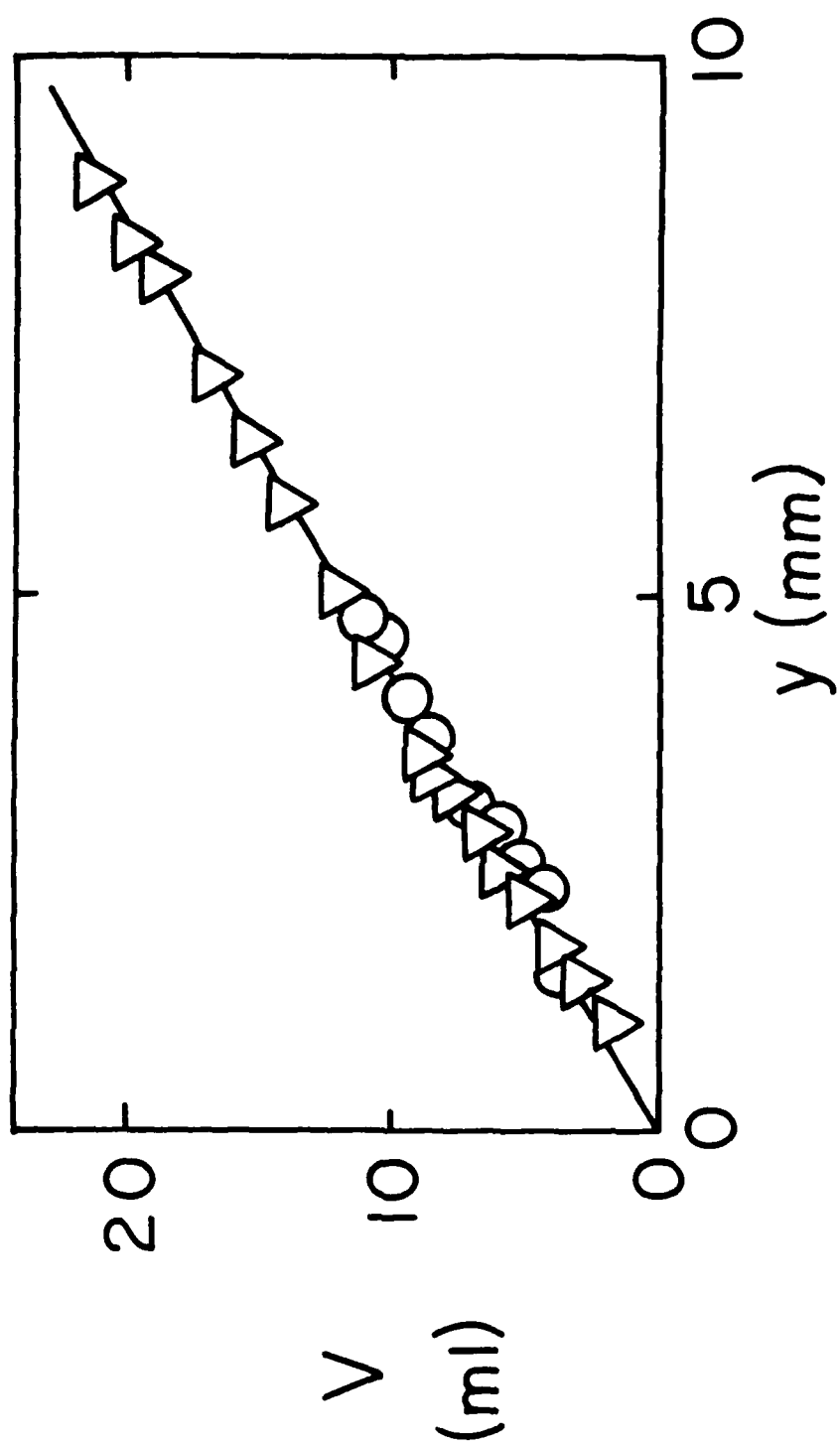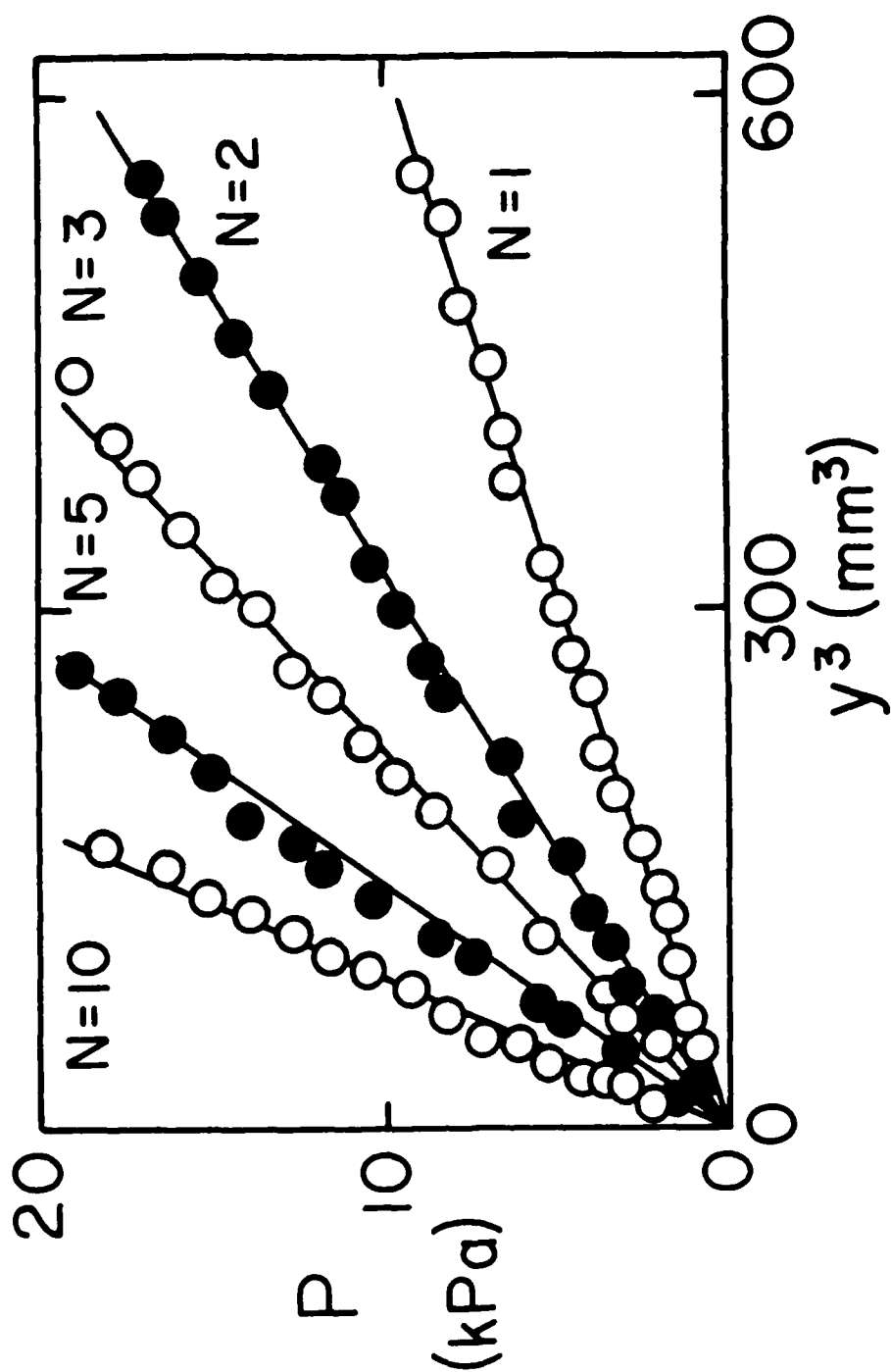   is of the theoretical form; $Pa = constant$, equation A.10.
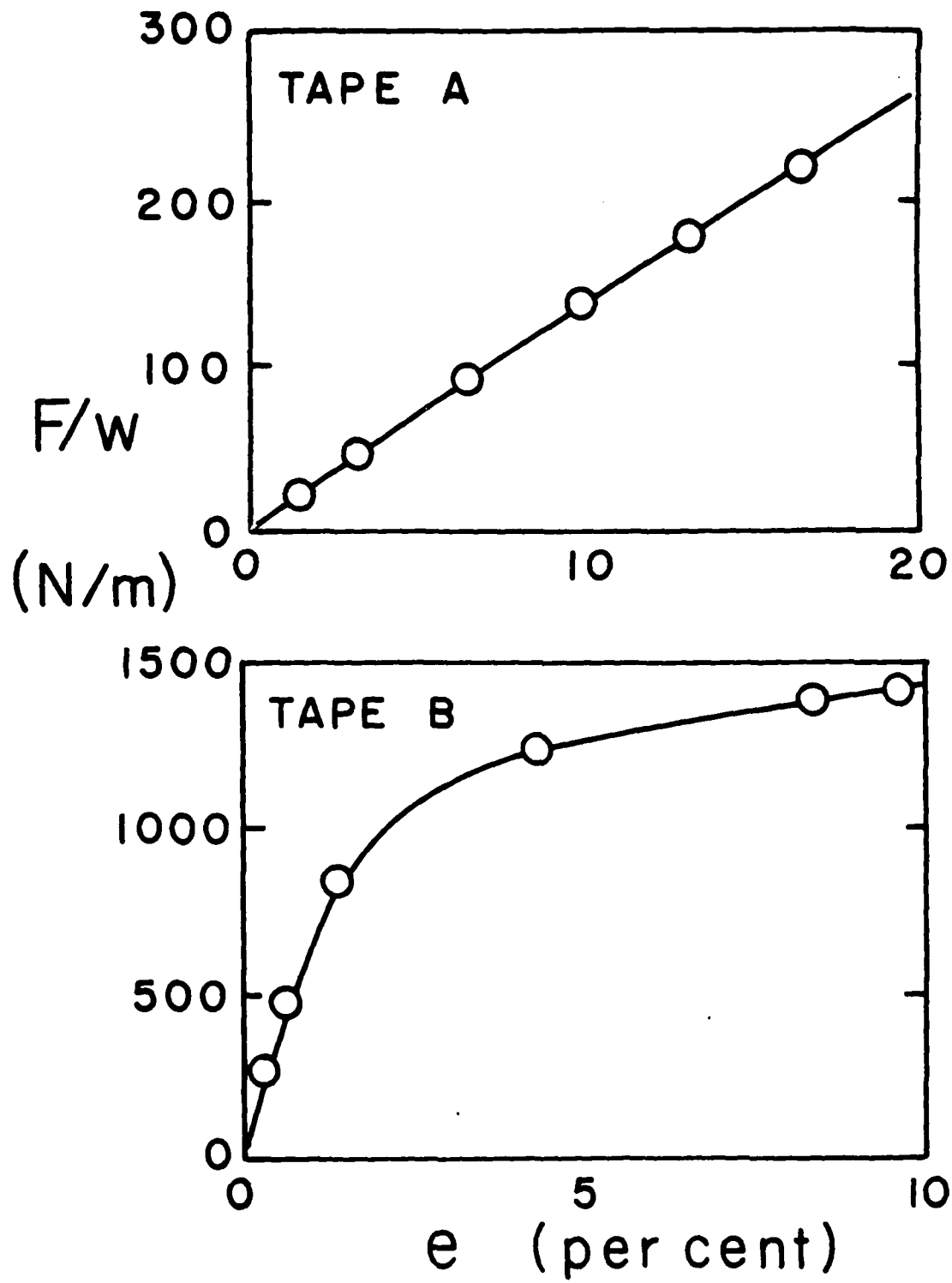
Figure 1

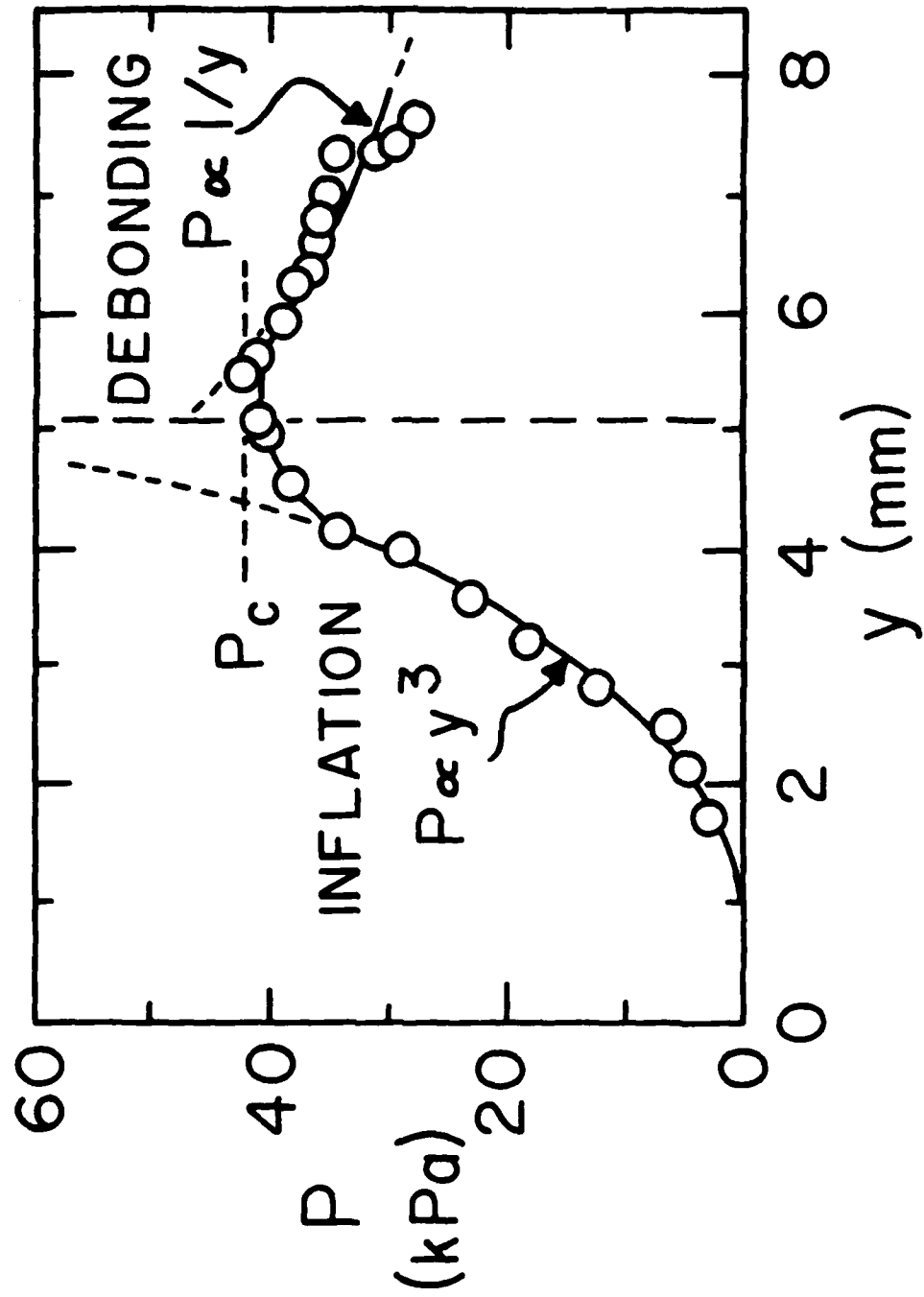Figure 2
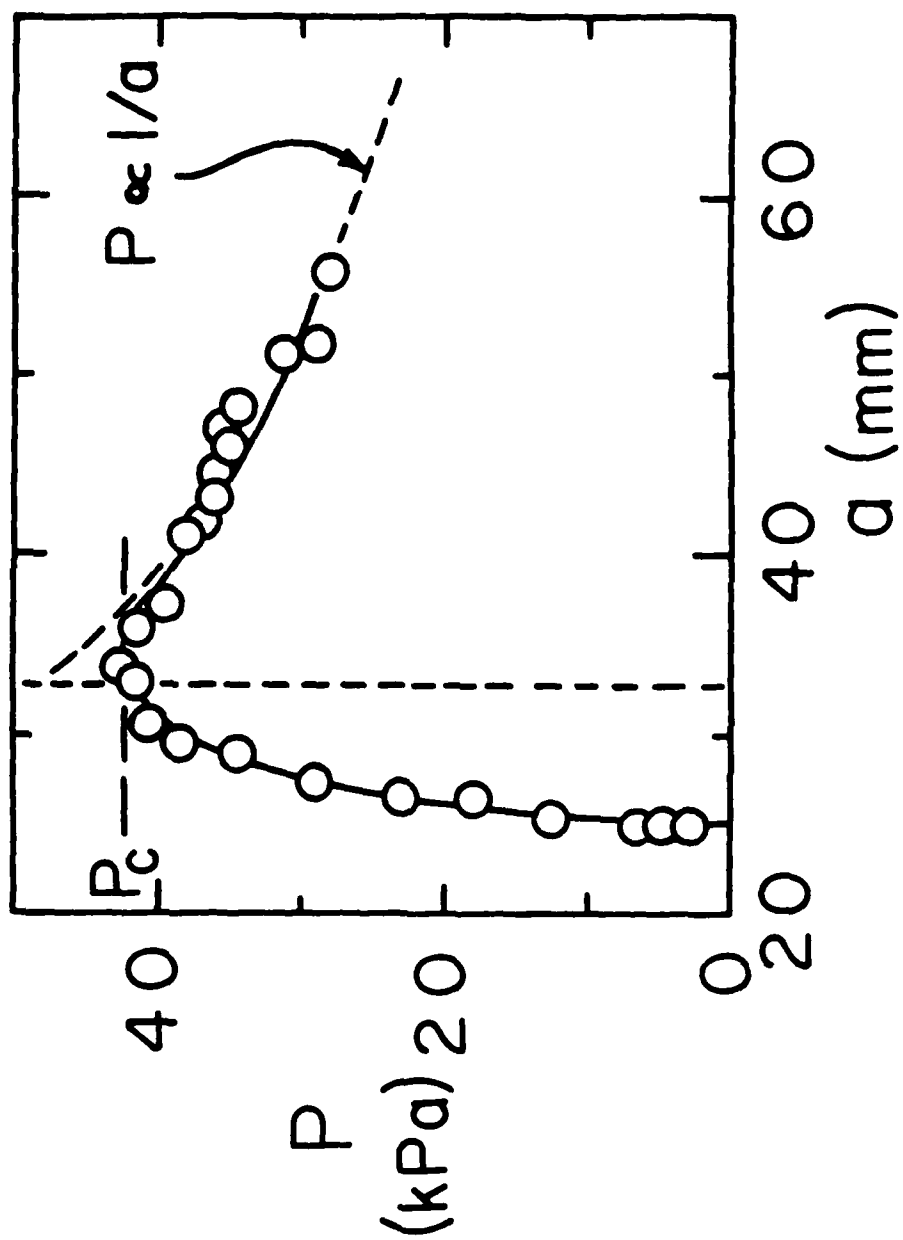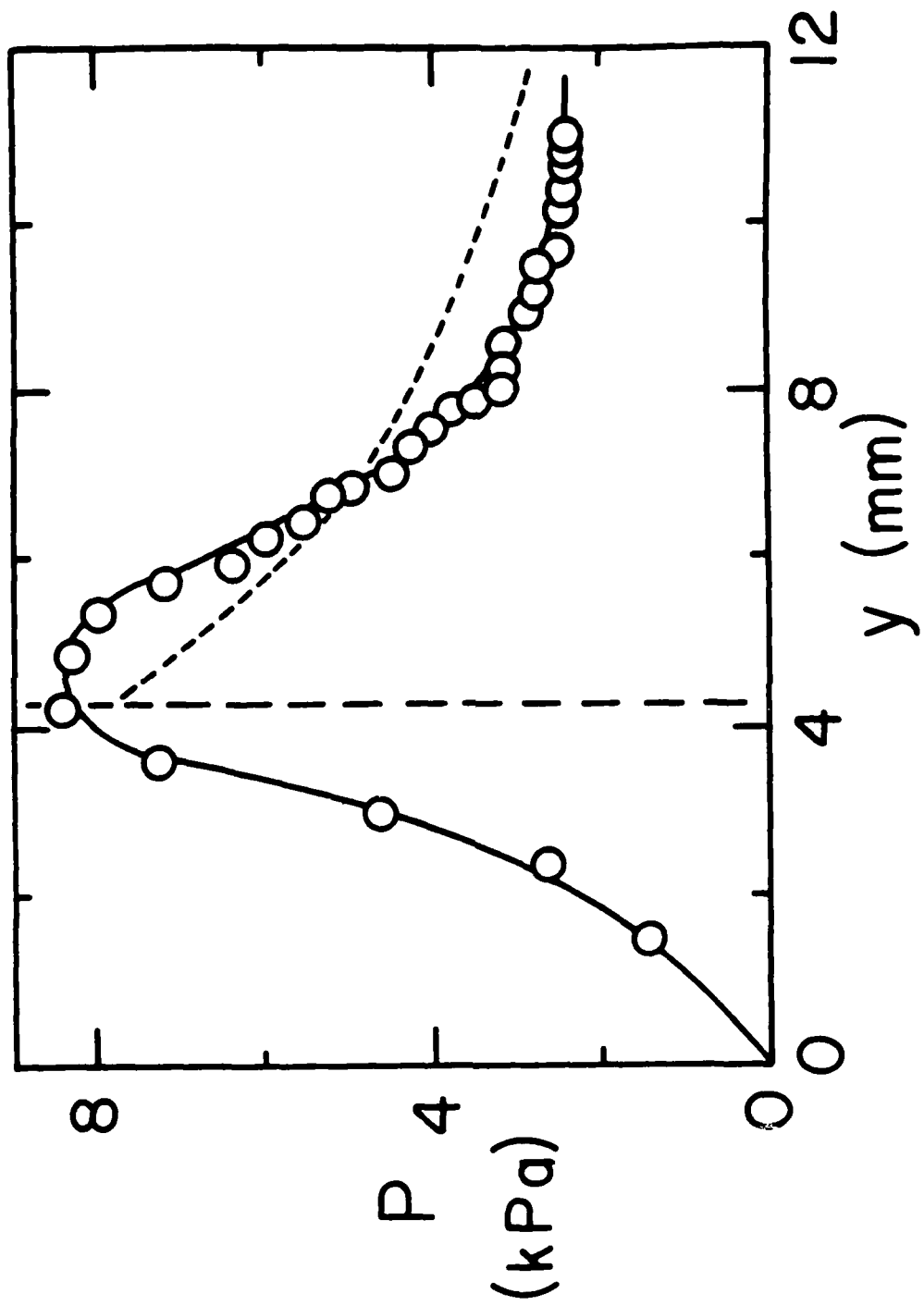
Figure 3

24

Figure 4

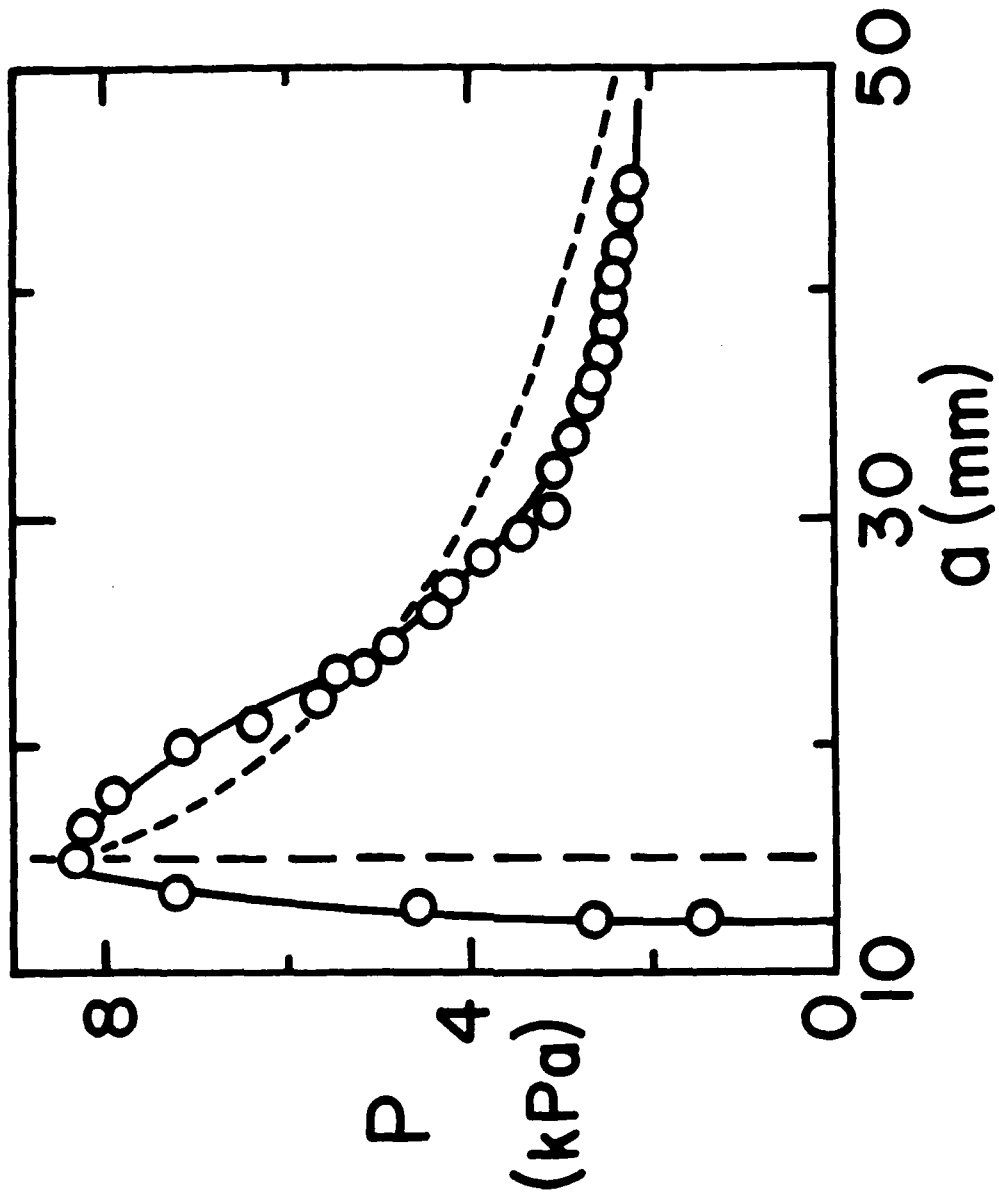Figure 5

Figure 6

Figure 7

Figure 8

(DYN)

DISTRIBUTION LIST

Dr. R.S. Miller
Office of Naval Research
Code 432P
Arlington, VA 22217
(10 copies)

Dr. J. Pastine
Naval Sea Systems Command
Code 06R
Washington, DC 20362

Dr. Kenneth D. Hartman
Hercules Aerospace Division
Hercules Incorporated
Alleghany Ballistic Lab
P.O. Box 210
Washington, DC 21502

Mr. Otto K. Heiney
AFATL-DLJG
Elgin AFB, FL 32542

Dr. Merrill K. King
Atlantic Research Corp.
5390 Cherokee Avenue
Alexandria, VA 22312

Dr. R.L. Lou
Aerojet Strategic Propulsion Co.
Bldg. 05025 - Dept 5400 - MS 167
P.O. Box 15699C
Sacramenta, CA 95813

Dr. R. Olsen
Aerojet Strategic Propulsion Co.
Bldg. 05025 - Dept 5400 - MS 167
P.O. Box 15699C
Sacramento, CA 95813

Dr. Randy Peters
Aerojet Strategic Propulsion Co.
Bldg. 05025 - Dept 5400 - MS 167
P.O. Box 15699C
Sacramento, CA 95813

Dr. D. Mann
U.S. Army Research Office
Engineering Division
Box 12211
Research Triangle Park, NC 27709-2211

Dr. L.V. Schmidt
Office of Naval Technology
Code 07CT
Arlington, VA 22217

JHU Applied Physics Laboratory
ATTN: CPIA (Mr. T.W. Christian)
Johns Hopkins Rd.
Laurel, MD 20707

Dr. R. McGuire
Lawrence Livermore Laboratory
University of California
Code L-324
Livermore, CA 94550

P.A. Miller
736 Leavenworth Street, #6
San Francisco, CA 94109

Dr. W. Moniz
Naval Research Lab.
Code 6120
Washington, DC 20375

Dr. K.F. Mueller
Naval Surface Weapons Center
Code R11
White Oak
Silver Spring, MD 20910

Prof. M. Nicol
Dept. of Chemistry & Biochemistry
University of California
Los Angeles, CA 90024

Mr. L. Roslund
Naval Surface Weapons Center
Code R10C
White Oak, Silver Spring, MD 20910

Dr. David C. Sayles
Ballistic Missile Defense
Advanced Technology Center
P.O. Box 1500
Huntsville, AL 35807

(DYN)

DISTRIBUTION LIST

Mr. R. Geisler
ATTN: DY/MS-24
AFRPL
Edwards AFB, CA 93523

Naval Air Systems Command
ATTN: Mr. Bertram P. Sobers
        NAVAIR-320G
Jefferson Plaza 1, RM 472
Washington, DC 20361

R.B. Steele
Aerojet Strategic Propulsion Co.
P.O. Box 15699C
Sacramento, CA 95813

Mr. M. Stosz
Naval Surface Weapons Center
Code R10B
White Oak
Silver Spring, MD 20910

Mr. E.S. Sutton
Thiokol Corporation
Elkton Division
P.O. Box 241
Elkton, MD 21921

Dr. Grant Thompson
Morton Thiokol, Inc.
Wasatch Division
MS 240 P.O. Box 524
Brigham City, UT 84302

Dr. R.S. Valentini
United Technologies Chemical Systems
P.O. Box 50015
San Jose, CA 95150-0015

Dr. R.F. Walker
Chief, Energetic Materials Division
DRSMC-LCE (D), B-3022
USA ARDC
Dover, NJ 07801

Dr. Janet Wall
Code 012
Director, Research Administration
Naval Postgraduate School
Monterey, CA 93943

Director
US Army Ballistic Research Lab.
ATTN: DRXBR-IBD
Aberdeen Proving Ground, MD 21005

Commander
US Army Missile Command
ATTN: DRSMI-RKL
        Walter W. Wharton
Redstone Arsenal, AL 35898

Dr. Ingo W. May
Army Ballistic Research Lab.
ARRADCOM
Code DRXBR - 1BD
Aberdeen Proving Ground, MD 21005

Dr. E. Zimet
Office of Naval Technology
Code 071
Arlington, VA 22217

Dr. Ronald L. Derr
Naval Weapons Center
Code 389
China Lake, CA 93555

T. Boggs
Naval Weapons Center
Code 389
China Lake, CA 93555

Lee C. Estabrook, P.E.
Morton Thiokol, Inc.
P.O. Box 30058
Shreveport, Louisiana 71130

Dr. J.R. West
Morton Thiokol, Inc.
P.O. Box 30058
Shreveport, Louisiana 71130

Dr. D.D. Dillehay
Morton Thiokol, Inc.
Longhorn Division
Marshall, TX 75670

G.T. Bowman
Atlantic Research Corp.
7511 Wellington Road
Gainesville, VA 22065

(DYN)

DISTRIBUTION LIST

R.E. Shenton
Atlantic Research Corp.
7511 Wellington Road
Gainesville, VA 22065

Mike Barnes
Atlantic Research Corp.
7511 Wellington Road
Gainesville, VA 22065

Dr. Lionel Dickinson
Naval Explosive Ordinance
Disposal Tech. Center
Code D
Indian Head, MD 20340

Prof. J.T. Dickinson
Washington State University
Dept. of Physics 4
Pullman, WA 99164-2814

M.H. Miles
Dept. of Physics
Washington State University
Pullman, WA 99164-2814

Dr. T.F. Davidson
Vice President, Technical
Morton Thiokol, Inc.
Aerospace Group
110 North Wacker Drive
Chicago, Illinois 60606

Mr. J. Consaga
Naval Surface Weapons Center
Code R-16
Indian Head, MD 20640

Naval Sea Systems Command
ATTN: Mr. Charles M. Christensen
        NAVSEA-62R2
Crystal Plaza, Bldg. 6, Rm 806
Washington, DC 20362

Mr. R. Beauregard
Naval Sea Systems Command
SEA 64E
Washington, DC 20362

Brian Wheatley
Atlantic Research Corp.
7511 Wellington Road
Gainesville, VA 22065

Mr. G. Edwards
Naval Sea Systems Command
Code 62R32
Washington, DC 20362

C. Dickinson
Naval Surface Weapons Center
White Oak, Code R-13
Silver Spring, MD 20910

Prof. John Deutch
MIT
Department of Chemistry
Cambridge, MA 02139

Dr. E.H. deButts
Hercules Aerospace Co.
P.O. Box 27408
Salt Lake City, UT 84127

David A. Flanigan
Director, Advanced Technology
Morton Thiokol, Inc.
Aerospace Group
110 North Wacker Drive
Chicago, Illinois 60606

Dr. L.H. Caveny
Air Force Office of Scientific
Research
Directorate of Aerospace Sciences
Bolling Air Force Base
Washington, DC 20332

W.G. Roger
Code 5253
Naval Ordance Station
Indian Head, MD 20640

Dr. Donald L. Ball
Air Force Office of Scientific
Research
Directorate of Chemical &
Atmospheric Sciences
Bolling Air Force Base
Washington, DC 20332

(DYN)

<u>DISTRIBUTION LIST</u>

Dr. Anthony J. Matuszko
Air Force Office of Scientific Research
Directorate of Chemical & Atmospheric
Sciences
Bolling Air Force Base
Washington, DC 20332

Dr. Michael Chaykovsky
Naval Surface Weapons Center
Code R11
White Oak
Silver Spring, MD 20910

J.J. Rocchio
USA Ballistic Research Lab.
Aberdeen Proving Ground, MD 21005-5066

G.A. Zimmerman
Aerojet Tactical Systems
P.O. Box 13400
Sacramento, CA 95813

B. Swanson
INC-4 MS C-346
Los Alamos National Laboratory
Los Alamos, New Mexico 87545

Dr. James T. Bryant
Naval Weapons Center
Code 3205B
China Lake, CA 93555

Dr. L. Rothstein
Assistant Director
Naval Explosives Dev. Engineering Dept.
Naval Weapons Station
Yorktown, VA 23691

Dr. M.J. Kamlet
Naval Surface Weapons Center
Code R11
White Oak, Silver Spring, MD 20910

Dr. Henry Webster, III
Manager, Chemical Sciences Branch
ATTN: Code 5063
Crane, IN 47522

Dr. A.L. Slafkosky
Scientific Advisor
Commandant of the Marine Corps
Code RD-1
Washington, DC 20380

Dr. H.G. Adolph
Naval Surface Weapons Center
Code R11
White Oak
Silver Spring, MD 20910

U.S. Army Research Office
Chemical & Biological Sciences
Division
P.O. Box 12211
Research Triangle Park, NC 27709

G. Butcher
Hercules, Inc.
MS X2H
P.O. Box 98
Magna, Utah 84044

W. Waesche
Atlantic Research Corp.
7511 Wellington Road
Gainesville, VA 22065

Dr. John S. Wilkes, Jr.
FJSRL/NC
USAF Academy, CO 80840

Dr. H. Rosenwasser
AIR-320R
Naval Air Systems Command
Washington, DC 20361

Dr. Joyce J. Kaufman
The Johns Hopkins University
Department of Chemistry
Baltimore, MD 21218

Dr. A. Nielsen
Naval Weapons Center
Code 385
China Lake, CA 93555

(DYN)

DISTRIBUTION LIST

K.D. Pae
High Pressure Materials Research Lab.
Rutgers University
P.O. Box 909
Piscataway, NJ   08854

Dr. John K. Dienes
T-3, B216
Los Alamos National Lab.
P.O. Box 1663
Los Alamos, NM   87544

A.N. Gent
Institute Polymer Science
University of Akron
Akron, OH   44325

Dr. D.A. Shockey
SRI International
333 Ravenswood Ave.
Menlo Park, CA   94025

Dr. R.B. Kruse
Morton Thiokol, Inc.
Huntsville Division
Huntsville, AL   35807-7501

G. Butcher
Hercules, Inc.
P.O. Box 98
Magna, UT   84044

W. Waesche
Atlantic Research Corp.
7511 Wellington Road
Gainesville, VA   22065

Dr. R. Bernecker
Naval Surface Weapons Center
Code R13
White Oak
Silver Spring, MD   20910

Prof. Edward Price
Georgia Institute of Tech.
School of Aerospace Engineering
Atlanta, GA   30332

J.A. Birkett
Naval Ordnance Station
Code 5253K
Indian Head, MD   20640

Prof. R.W. Armstrong
University of Maryland
Dept. of Mechanical Engineering
College Park, MD   20742

Herb Richter
Code 385
Naval Weapons Center
China Lake, CA   93555

J.T. Rosenberg
SRI International
333 Ravenswood Ave.
Menlo Park, CA   94025

G.A. Zimmerman
Aeroject Tactical Systems
P.O. Box 13400
Sacramento, CA   95813

Prof. Kenneth Kuo
Pennsylvania State University
Dept. of Mechanical Engineering
University Park, PA   16802

T.L. Boggs
Naval Weapons Center
Code 3891
China Lake, CA   93555

(DYN)

DISTRIBUTION LIST

Dr. C.S. Coffey
Naval Surface Weapons Center
Code R13
White Oak
Silver Spring, MD   20910

D. Curran
SRI International
333 Ravenswood Avenue
Menlo Park, CA   94025

E.L. Throckmorton
Code SP-2731
Strategic Systems Program Office
Crystal Mall #3, RM 1048
Washington, DC   23076

Dr. R. Martinson
Lockheed Missiles and Space Co.
Research and Development
3251 Hanover Street
Palo Alto, CA   94304

C. Gotzmer
Naval Surface Weapons Center
Code R-11
White Oak
Silver Spring, MD   20910

G.A. Lo
3251 Hanover Street
B204 Lockheed Palo Alto Research Lab
Palto Alto, CA   94304

R.A. Schapery
Civil Engineering Department
Texas A&M University
College Station, TX   77843

J.M. Culver
Strategic Systems Projects Office
SSPO/SP-2731
Crystal Mall #3, RM 1048
Washington, DC   20376

Prof. G.D. Duvall
Washington State University
Department of Physics
Pullman, WA   99163

Dr. E. Martin
Naval Weapons Center
Code 3858
China Lake, CA   93555

Dr. M. Farber
135 W. Maple Avenue
Monnovia, CA   91016

W.L. Elban
Naval Surface Weapons Center
White Oak, Bldg. 343
Silver Spring, MD   20910

G.E. Manser
Morton Thickol
Wasatch Division
P.O. Box 524
Brigham City, UT   84302

R.G. Rosemeier
Brimrose Corporation
7720 Belair Road
Baltimore, MD   20742

Administrative Contracting   Director
  Officer (see contract for   Naval Research Laboratory
  address)   Attn: Code 2627
(1 copy)   Washington, DC   20375
                                        (6 copies)

Defense Technical Information Center
Bldg. 5, Cameron Station
Alexandria, VA   22314
(12 copies)

Dr. Robert Polvani   Dr. Y. Gupta
National Bureau of Standards   Washington State University
Metallurgy Division   Department of Physics
Washington, D.C.   20234   Pullman, WA   99163

END

12-86

DTIC